Biochimica et Biophysica Acta 859 (1986) 33–48
Elsevier

BBA 73140

Morphological changes of phosphatidylcholine bilayers induced by melittin: vesicularization, fusion, discoidal particles

Jean Dufourcq [a], Jean-Francois Faucon [a], Georges Fourche [a], Jean-Louis Dasseux [a], Marc Le Maire [b] and Thaddée Gulik-Krzywicki [b]

[a] *Centre de Recherche Paul Pascal, CNRS, Domaine Universitaire, 33405 Talence Cedex and* [b] *Centre de Genetique Moléculaire CNRS, 91190 Gif sur Yvette Cedex (France)*

(Received February 10th 1986)

Key words Melittin, Phosphatidylcholine bilayer, Discoidal particle, Light scattering, Freeze-fracture electron microscopy, Membrane morphology

Morphological changes induced by the melittin tetramer on bilayers of egg phosphatidylcholine and dipalmitoylphosphatidylcholine have been studied by quasi-elastic light scattering, gel filtration and freeze-fracture electron microscopy. It is concluded that melittin similarly binds and changes the morphology of both single and multilamellar vesicles, provided that their hydrocarbon chains have a disordered conformation, i.e , at temperatures higher than that of the transition, T_m. When the hydrocarbon chains are ordered (gel phase), only small unilamellar vesicles are morphologically affected by melittin. However after incubation at $T > T_m$, major structural changes are detected in the gel phase, regardless of the initial morphology of the lipids Results from all techniques agree on the following points (i) At low melittin content, phospholipid-to-peptide molar ratios, $R_t > 30$, heterogeneous systems are observed, the new structures coexisting with the original ones. (ii) For lipids in the fluid phase and $R_t > 12$, the complexes formed are large unilamellar vesicles of about 1300 ± 300 Å diameter and showing on freeze-fracture images rough fracture surfaces. (iii) For lipids in the gel phase, $T < T_m$ after passage above T_m, and for $5 < R_t < 50$, disc-like complexes are observed and isolated. They have a diameter of 235 ± 23 Å and are about one bilayer thick; their composition corresponds to one melittin for about 20 ± 2 lipid molecules. It is proposed that the discs are constituted by about 1500 lipid molecules arranged in a bilayer and surrounded by a belt of melittin in which the mellitin rods are perpendicular to the bilayer. (iv) For high amounts of melittin, $R_t < 2$, much smaller and more spherical objects are observed. They are interpreted as corresponding to lipid-peptide comicelles in which probably no more bilayer structure is left. It is concluded that melittin induces a reorganization of lipid assemblies which can involve different processes, depending on experimental conditions: (i) vesicularization of multibilayers; (ii) fusion of small lipid vesicles; (iii) fragmentation into discs and micelles. Such processes are discussed in connexion with the mechanism of action of melittin: the lysis of biological membranes and the synergism between melittin and phospholipases.

Introduction

Despite intensive studies on melittin-phospholipid systems, our knowledge of the real mechanism of lysis, or morphological perturbations of

Abbreviations DPPC, dipalmitoylphosphatidylcholine egg PC, egg phosphatidylcholine, SUV, sonicated unilamellar vesicles MLV, multilamellar dispersion R_t, phospholipid-to-melittin molar ratio R_c, phospholipid to melittin molar ratio in the complexes

bilayers and membranes, induced by this amphipathic peptide is still scarce and controversial This is in spite of interesting results already obtained on the structure and the dynamics of the peptide [1–3], lipids [4–6] and their interactions [7,8] Since the early study by Sessa et al [9], it is well established that melittin increases the permeability of liposomes to small solutes and that some fragmentation of bilayers can be detected by negative staining electron microscopy More recently, several authors have mentioned a clearing of lipid dispersions in the presence of large amounts of the peptide and at high concentration [5,10] However, until the work of Prendergast et al [11], no attempt was made to characterize such lipid-melittin complexes These authors showed by light scattering that melittin induces several changes in the diameter of lipid vesicles of dimyristoyl- and dipentadecanoylphosphatidylcholine However, several points in this study are questionable due to the degradation of lipids by residual phospholipase activity [5,6] In order to clarify this situation and, at the same time, obtain precise information on the nature of morphological changes induced by melittin on lipids, we have undertaken a combined light scattering, gel-filtration and freeze-fracture electron microscopy study on melittin-phosphatidylcholine systems (egg and dipalmitoyl)

The results obtained allow us to answer two important questions

(i) Does melittin induce small size lipid-peptide complexes and, if so, what is their structure?

(ii) Does melittin induce a general reorganisation of lipid bilayers, in connection with the recently documented fusion of vesicles [12,13]?

Materials and Methods

Melittin used throughout this study was either purified by HPLC as already described [5] or obtained from Bachem Feinchemikalien AG (Switzerland) and used without further purification In all cases, EDTA was added in order to inhibit any possible residual phospholipase activity Most of the experiments were done with melittin of both origins and gave identical results

Dipalmitoylphosphatidylcholine (DPPC) was from Sigma or Medmark (Darmstadt, F G R) The lipid dispersions (MLV) were effected by hydration of the dried lipids with 20 mM phosphate buffer at $T > T_m$ and vortexing The vesicles (SUV) were obtained by sonication for 5 min at $T > T_m$ with an Annemasse F50 sonicator

For freeze-fracture electron microscopy, the samples were prepared in a 100 mM phosphate buffer (pH 7 5), 10 mM EDTA, containing 25–30% glycerol The final DPPC concentration was kept constant at 15 mM and the amount of melittin was varied accordingly to obtain the desired R_1 (R_1 is the molar ratio Phospholipid/peptide in the incubation mixtures) The small drops of preparations were deposited on conventional Balzers gold planchet and rapidly frozen in liquid propane Fracturing and replication were performed using a Balzers BAF 301 freeze-etching unit equipped with an electron gun for platinum-carbon shadowing The replicas, after digestion of organic material with chromic acid and washing with distilled water, were examined in a Philips 301 electron microscope In order to estimate quantitatively the size and volume occupied by the objects, several photographs with several hundreds objects from different experiments were treated [14] The experimental total volume occupied was defined as $V = (\bar{D}/2)^3 \times 4\pi/3 \times N_v$, where $\bar{D}$ is the average diameter of the objects and N_v the average number of objects per unit volume [14] The partial specific volumes of melittin and DPPC, 0 75 and 0 975 cm^3/g, respectively, allowed calculation of the total volume of objects

Gel-filtration experiments were done on a 40 × 1 5 cm Sepharose 4B column at constant temperatures of 10 and 20°C The column was equilibrated and loaded with 10 mg of pure DPPC in order to improve the recovery of the lipids The flow rate was about 8 ml/h and 1–1 4 ml fractions were collected The column was calibrated with blue dextran, thyroglobulin, catalase and carboxyfluorescein The calibration curve which fitted that expected [15], permitted estimation of the hydrodynamic radius, R_H (Stokes radius), of the species Experiments were also performed at 10°C on a 20 × 1 2 cm Sephadex G-50 column in order to separate lipid-melittin complexes quickly from free peptide In the eluate, the concentration of melittin (M_r 2840 for the monomer) was determined (i) by absorption $\epsilon_{280} = 5600\ M^{-1}$

cm^{-1} after subtraction of the eventual scattering contribution calculated by extrapolation of the scattering in the 650–350 mn range, (ii) by fluorescence at 360 nm, at this wavelength the quantum yield is the same for free and bound melittin under the conditions used herein [16] Phospholipid content was estimated by ^{14}C radioactivity measured by liquid scintillation counting This allowed calculation of the real molar ratio of both components within the complexes, R_c = phospholipid/melittin

Light-scattering changes at 90° were first monitored using a classical spectrofluorometer Quantitative measurements were carried out by quasi-elastic light scattering using a Krypton ion laser at $\lambda_0 = 647$ nm (Spectra Physics series 2000) The correlation function of the scattered light was recorded at 90° angle with fast clipped real time correlator (ATNE, Paris, France) with 100 channels and a time resolution of 10 ns The homodyne detection of the scattered light was performed with a digital photon counting device (Malvern Instruments, U K) Correlation times were measured with a 10% accuracy taking into account both the deviations from the technique and the reproducibility from sample to sample The autocorrelation function of the scattered light was fitted using the method of cumulants [17]

In order to calibrate the size of particles, uniform polystyrene latex beads of known diameter, 380 ± 25 and 800 ± 40 Å, from Interchim were used both in quasi-elastic light scattering and freeze-fracture measurements

Results

Morphological changes detected by light scattering

When melittin is added at a molar ratio $R_i \cong 20$ to DPPC dispersions in their gel phase (4°C), no change in the light scattering is detected Conversely, no change in the fluorescence of melittin is detected, indicating that no interaction occurs However, when the temperature of that mixture is increased, as shown in Fig 1, the scattered intensity severely decreases at temperatures $T > 30$°C down to a plateau value obtained in the fluid phase, i e $T > 41$°C When the temperature of the same sample is decreased, a new decrease in the scattered intensity occurs below 41°C Then, at room temperature, a dramatic clearing effect of the initial dispersion is obtained Further heating and cooling scans are superimposed, indicating that no further change on the overall shape of particles occurs in the time scale of a few hours When similar experiments are done using higher amounts of melittin, as shown in Fig 1 for $R_i = 2$, the clearing of the solution also appears on the first heating through the transition domain How-

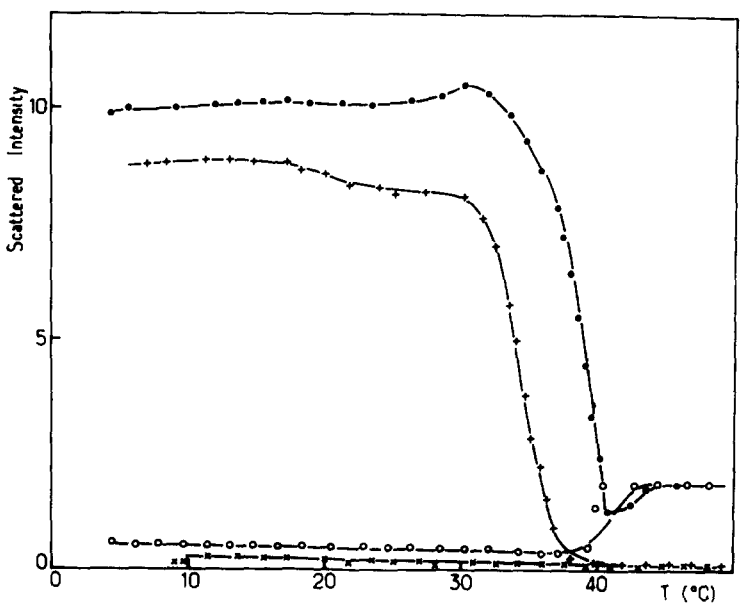

Fig 1 Light scattered intensity at 480 nm versus temperature for DPPC dispersions in the presence of different amounts of melittin Peptide is added at 4°C to the preformed dispersions $R_i = 20$ ●, first heating, ○ cooling and consecutive scans $R_i = 2$ + first heating, ×, cooling and consecutive scans 20 mM phosphate buffer, 1 mM EDTA (pH 7 5), [DPPC] = 8 mM

ever, on decreasing temperature and for any further scan, no more change can be detected, the solution remaining totally clear whatever the temperature

A more quantitative study of this system has been performed by quasi-elastic light scattering, and the results obtained at 21°C after incubation of the sample at 50°C are plotted on Fig 2 Dispersions of DPPC can be analyzed as large species of 1 3–1 5 μm radius The addition of small amounts of melittin induces an increase in their apparent size up to about 3 μm for $R_i = 50$, followed by a decrease in R_H for lower R_i values (Fig 2) The system becomes quite heterogeneous for R_i values lower than $R_i = 40$ In order to check for the presence of small objects, such systems have also been investigated after low-speed centrifugation (10 min at 6000 × g) which pellets the large particles As shown in Fig 2, small objects remain in the supernatant, their size increasing from $R_H = 430$ Å up to about 2800 Å for $R_i = 100$ Further addition of melittin results in a drastic decrease in the size down to $R_H = 150$–200 Å for $R_i = 50$, followed by a monotonous decrease of R_H down to a limiting value $R_H = 80$ Å at $R_i = 5$ For $R_i < 13$, large particles of several micrometers completely vanish, and the correlation decays are reasonably well fitted by a single exponential Despite observation of heterogeneous systems above $R_i = 13$, one has to mention that in both cases, with and without centrifugation, melittin first induces an increase in the size of species before decreasing it drastically for $50 < R_i < 100$

Since the hydrocarbon chains of egg PC are, at the temperature of experiments, in the fluid α conformation, no incubation at higher temperatures was needed to study the effect of melittin on egg PC dispersions behaviour Dispersions of egg PC are also detected as large objects of about 1 6 μm (Fig 2) The addition of melittin results directly in a very drastic decrease of R_H up to $R_i = 25$, then R_H remains almost constant, at 1700 Å, for $13 < R_i < 25$, as seen in Fig 2 When more melittin is added, at $R_i < 13$, a new sharp decrease in R_H is observed from $R_H = 1700$ Å down to $R_H \cong 150$ Å Further addition of melittin results in a progressive decrease down to $R_H = 80$ Å for $R_i = 7$ After looking at the effect of lipid chains in different states, in the liquid crystalline

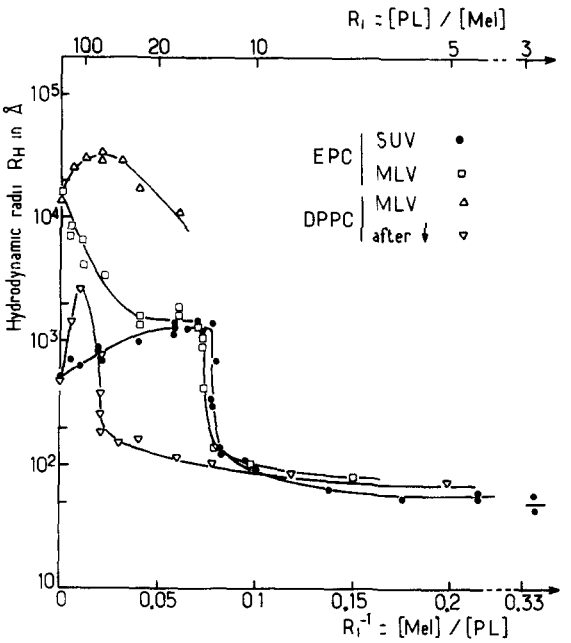

Fig 2 Hydrodynamic radii, R_H of lipid-peptide systems versus R_i, for lipids in different physical states, obtained by quasi-elastic light scattering Initial state of the lipids EPC sonicated vesicles (●), EPC multilamellar dispersions (□) DPPC multilamellar dispersions (△), similar but after centrifugation of the peptide-lipid system (▽) 20 mM phosphate buffer/1 mM EDTA (pH 7 5) Phospholipid concentration was 2 6 mM, temperature, 21°C

and gel phase for dispersions egg PC and DPPC, respectively, it was interesting to document the behaviour of melittin towards morphologically different systems, i e , sonicated vesicles As shown in Fig 2, egg PC vesicles which have an initial size $R_H \cong 540$ Å, increase their hydrodynamic radius up to $R_H \cong 1400$ Å when melittin is added up to $R_i = 17$, then R_H remains constant up to $R_i = 13$ Further addition of melittin again drastically decreases R_H down to about 150 Å for $R_i = 12$ Interestingly such a sharp decrease is similar to that already found for egg PC dispersions (Fig 2) Finally, increasing melittin amounts up to $R_i = 3$ results only in a smooth variation of R_H followed by a plateau corresponding to $R_H \cong 50$ Å The static scattered intensity has also been measured independently it first increases 4-fold when melittin is added up to $R_i = 26$ and afterwards decreases for higher melittin amounts, but in a more progressive way compared to the sharp drop of

R_H value at $R_i = 13$ (data now shown)

In order to investigate the behaviour of melittin in the presence of low amounts of lipids, experiments were carried out by adding egg PC dispersions to a melittin solution For pure melittin, which is in the tetrameric structure, a value of $R_H = 20$ Å was found, this agrees with that proposed in the literature [18] Addition of lipids immediately results in an increase of R_H, 35 Å < R_H < 130 Å for 1 4 < R_i < 7, values in good agreement with those already found in Fig 2 At intermediate R_i values, 10 < R_i < 28, a plateau of R_H is observed which corresponds to $R_H \cong 1800$ Å, a value very close to that already found both for MLV and SUV in this intermediary range of R_i (data now shown)

The autocorrelation function, $g^{(2)}(\tau)$, was generally almost monoexponential, except in the regions where R_H values vary strongly This is illustrated in Fig 3, where the experimental decays are shown for two characteristic systems egg PC vesicles plus melittin at $R_i = 17$ (which corresponds to the intermediary plateau of R_H values already mentioned in Fig 2), and egg PC vesicles plus melittin at $R_i = 7$, relevant for small particles In these cases the cumulant method gives a good fit, with a relative variance, $\mu_2/\bar{\Gamma}^2$, of about 0 2, indicating a fairly homogeneous population

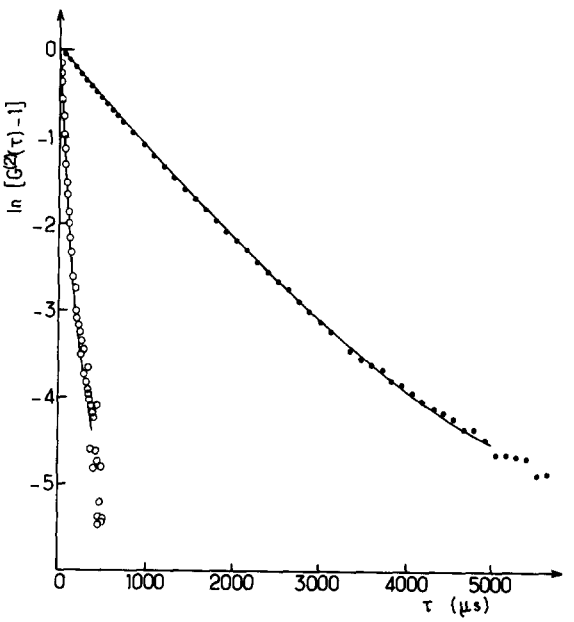

Fig 3 Autocorrelation functions of the scattered light for two representative systems of EPC vesicles in presence of melittin $R_i = 17$ (●) and $R_i = 7$ 4 (○), the continuous curves are calculated by the cumulant method 20 mM phosphate buffer/1 mM EDTA (pH 7 5), [EPC] = 2 6 mM, temperature, 21°C

Detection and analysis of lipid-peptide complexes by gel-filtration

Gel-filtration experiments were done on a calibrated Sepharose 4B column which permits analysis of changes in the size of SUV As shown in Fig 4, at 20°C, freshly prepared concentrated solution of DPPC sonicated vesicles (5–10 mg/ml) elute as a single major peak at $V_e = 20$ ml when detected by ^{14}C radioactivity A minor peak at the excluded volume, $V_0 = 10$ 8 ml, indicates the presence of small amounts of high-molecular-weight species, either agregated vesicles or non-dispersed lipids When melittin-DPPC complexes are formed by incubation at 50°C and then loaded on the column at 20°C for $R_i = 30$, a quite different pattern is observed the amount of lipids excluded at V_0 increases, while a new sharper peak elutes at $V_e = 21$ 8 ml From the calibration curve (cf Materials and Methods) one can deduce an hydrodynamic radius of the complexes, $R_H \cong 72$ Å, i e, particles smaller than the initial SUV of pure lipids When increasing the melittin content in the incubation mixture, this last peak becomes pre-

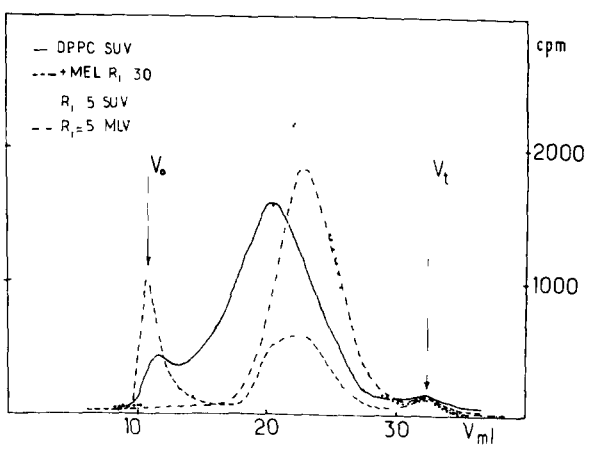

Fig 4 Elution profiles on Sepharose 4B of melittin-DPPC complexes followed by ^{14}C-labelled lipids 0 2 ml of the incubated mixtures were loaded onto the column, [DPPC] = 13 6 mM 100 mM phosphate buffer/1 mM EDTA (pH 7 5), temperature, $T = 22$°C V_0 and V_t are respectively the excluded and total volume of the column

dominant but remains sharp at almost the same elution volume $V_e = 22–23$ ml, corresponding to $R_H \cong 66–70$ Å At $R_i = 5$, as shown on Fig 4, only this lipid peak is detected, indicating that all the lipids are reorganized into small particles Similar experiments with DPPC dispersions incubated with melittin above T_m gave identical results (Fig 4)

When the elution profile is followed both for lipids and for the peptide (Fig 5) further conclusions can be drawn (i) a corresponding peak of melittin is coeluted with lipids at $V_e \cong 22–23$ ml, (ii) a peak of free melittin is well resolved at $V_e = 28$ ml, and its intensity increases with the amount of melittin in the incubation mixture Due to its concentration and buffer conditions, melittin elutes as a tetramer [19]

Fluorescence emission spectra of melittin along the elution profile compared to previous binding studies [16] confirm that melittin is free in solution in the latest peak, while it is bound to lipids in the first one

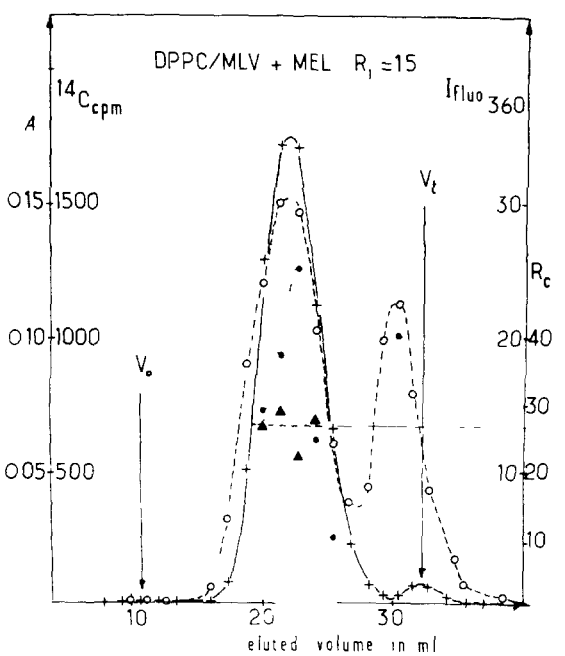

Fig 5 Elution profiles on Sepharose 4B of DPPC multilamellar dispersions incubated with melittin at $R_i = 15$ + ^{14}C radioactivity of lipids, ○, A at 280 nm, ●, fluorescence intensity at 360 nm (excitation 280 nm), △, R_c = molar ratio of DPPC to melittin in each fraction experimental conditions identical to those in Fig 4

Finally, the lipid-to-peptide molar ratio along the elution profile can be estimated from the concentrations of each reactants in all fractions (cf Materials and Methods) The obtained values of $R_c = [PL]/[mel]$ in the complexes are reasonably constant along the peak of small particles (Fig 5) This indicates the existence of a relatively well defined 'stoichiometry' for the complex with $R_c \cong 23$ for $5 < R_i < 15$ (Table I) The particles eluting at larger volumes, $V_e \cong 28$ ml, have $R_c < 1$, while for those eluting at V_0 (Fig 4) the R_c values ($R_c > 200$) are very high and not constant In an independent experiment, an aliquot of the DPPC-melittin complexes eluted at $V_e = 23$ ml was reloaded onto the same column Complexes were again eluted at $V = 23$ ml with an R_c value of the same order, but a peak at 28 ml corresponding to free melittin was detected, which shows that complexes slowly dissociated at 20°C on the column In order to limit such a dissociation of DPPC-melittin complexes, gel-filtration experiments were done on a G-50 Sephadex column On such a column, lipid-peptide complexes eluted at V_0, while free melittin was included, this allowed a separation in less than 10 min For R_i varying from 15 to 5, the complexes have almost a constant composition, $R_c \cong 18 \pm 2$

Experiments done with dimyristoyl- instead of dipalmitoylphosphatidylcholine at 20 and 10°C also indicated that small size particles can be formed in the presence of melittin for $R_i = 15$ and $R_i = 4$ when starting both from dispersions and from sonicated vesicles

Finally, experiments similar to those shown in Figs 4 and 5 were carried out with egg PC at 20°C, and quite similar results were observed However, at $R_i = 30$, most of the lipids elute at the excluded volume V_0, indicating that large-diameter particles are formed from SUV Conversely, at $R_i = 5$, mainly small-sized particles are eluted at $V_e = 27\,3$ ml, corresponding to $R_H \cong 37$ Å (Table I) Moreover, instead of the sharp peak of complexes observed with DPPC, the elution profiles with egg PC display a broad peak spread over a large domain of elution, which indicates a broad distribution of particles size From the respective contents of melittin and egg PC, the calculated values of R_c are shown to vary continuously through the peak of the egg PC-melittin

TABLE I

CHARACTERISTICS OF MELITTIN-PC COMPLEXES FRACTIONATED BY GEL-FILTRATION ON SEPHAROSE 4B AT $T = 20°C$ AFTER INCUBATION OF THE MIXTURES AT $T > T_m$

EPC, egg phosphatidylcholine, Mel, melittin

Experimental conditions			Elution volume (ml)	K_d	R_H (Å)	R_c = [PL]/[Mel]
Phase	Vesicle	R_t				
Gel phase	$DPPC_{SUV}$		20	0 42		
	$DPPC_{SUV}$-Mel	30	21	0 47	79	50 ± 20
	$DPPC_{MLV}$-Mel	15	22	0 52	70	24 ± 5
	$DPPC_{SUV}$-Mel	5	22 9	0 56	66	21 ± 5
	$DPPC_{MLV}$-Mel	5	22 9	0 56	66	25 ± 7
	[a]DMPC-Mel	3 6	23	0 56	68	15
Liquid crystal	EPC_{SUV}-Mel	30	26 4	0 71	44	
	EPC_{MLV}-Mel	15	25	0 66	51	
	EPC_{SUV}-Mel	5	27 3	0 76	37	
$T \cong T_m$	$DMPC_{MLV}$-Mel	15	21 6	0 5	74	25 ± 5
Pure Mel tetramer			30	0 88	20	

[a] At 10°C

complexes from 200 to about 10 on increasing elution volume Therefore a distribution in size and composition does exist, and this could be related to a more significant dissociation of the egg PC-melittin complexes on the column compared to those of DPPC

Structure of lipid-peptide complexes as revealed by freeze-fracture electron microscopy

Freeze-fracture electron microscopy is one of the most straightforward methods for studying lipid-water and protein-lipid-water systems, provided that the freezing of the samples is rapid enough to preserve their initial structure [20,21]

Freeze-fracture images of pure dispersions of DPPC show, at 20°C, large liposomes, formed by regularly stacked, smooth lamellae The addition of melittin, at $R_t = 30$, has no appreciable effect on the general morphology of this system (Fig 6A) Similar findings are observed up to $R_t = 5$ The differences appear only when samples are brought to 50°C, i e , when the hydrocarbon chains of DPPC are in the disordered, α, conformation Hardly any change is observed in the case of pure DPPC, while drastic changes, leading to the appearance of large unilamellar vesicles (Fig 6B), are observed in the presence of melittin at $R_t = 30$

When the samples are cooled down to 20°C, pure DPPC shows stacked lamellae, and DPPC-melittin sample shows a coexistence of flat lamellae (large arrows on Fig 6C) and some new, small and flat objects (Fig 6C, small arrows) The amount of lamellae decreases with increasing concentration of melittin, and, starting from $R_t = 15$, only small and flat objects are seen for the samples frozen from 20°C after the incubation at 50°C

For lower R_t values, the general shape of the objects seems to become more spherical and their apparent diameter decreases from 190 Å at $R_t = 15$ to 120 Å at $R_t = 2$ The total volumes occupied by these particles, calculated as described in Materials and Methods, are reported in Table II These values agree with those calculated using the molar volume of DPPC and melittin, assuming, in a first approximation, that the objects are filled spheres For extreme values of R_t, $R_t = 2$, the low amount of material detected, compared to that expected (Table II), probably indicates that a significant fraction of the material is not seen

When melittin is added to DPPC vesicles at 20°C, the initial vesicular material (Fig 7A) is transformed to less well defined mostly flat objects (Fig 7B), indicating a strong interaction be-

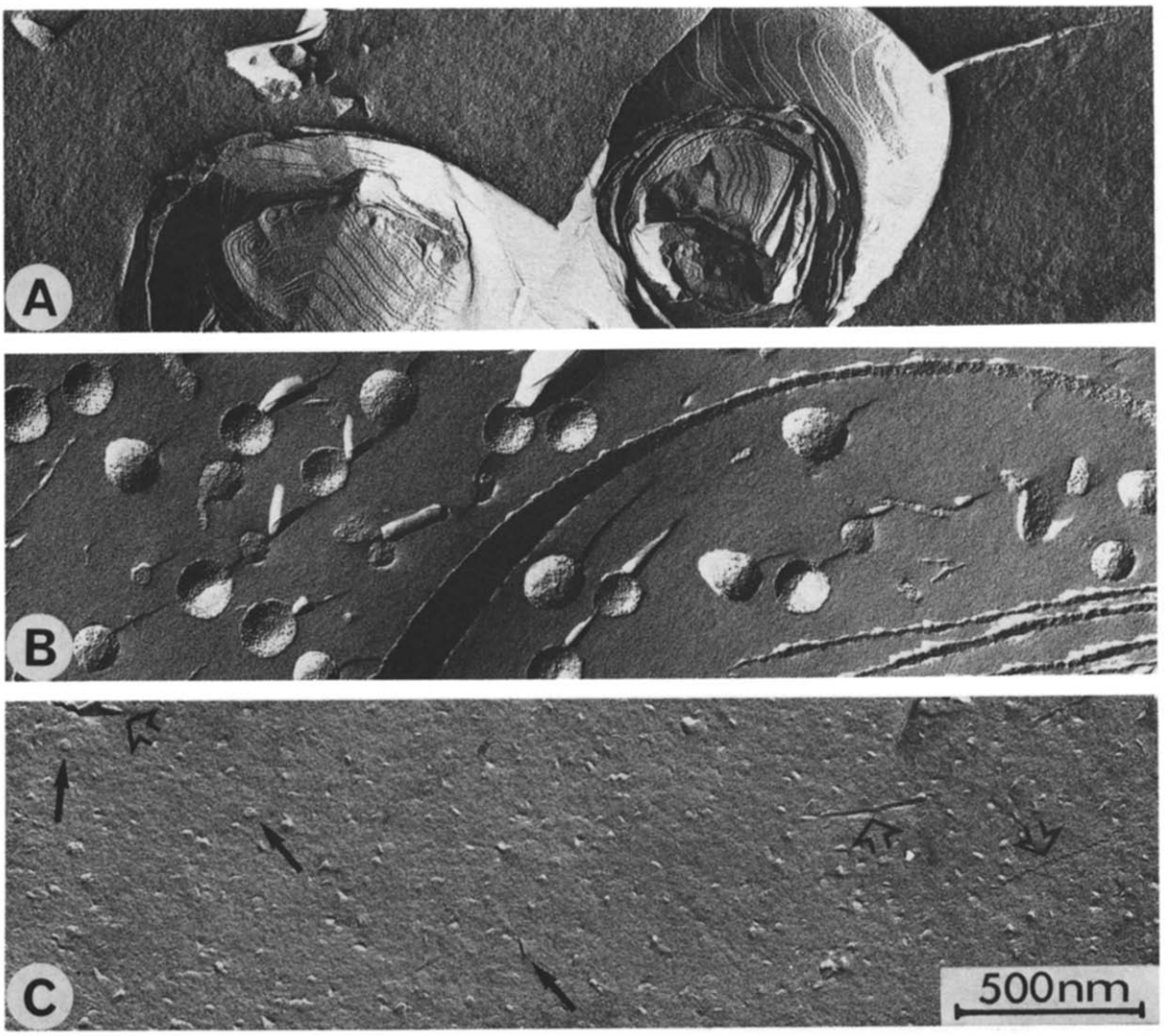

Fig 6 Freeze-fracture electron micrographs of DPPC dispersions in the presence of melittin $R_t = 30$, and at different temperature: (A) freeze-fractured from 20°C (B) freeze-fractured from 50°C (C) freeze-fractured from 20°C after incubation at 50°C

TABLE II

TOTAL VOLUME OCCUPIED BY OBJECTS DETECTED BY FREEZE-FRACTURE ELECTRON MICROSCOPY

	Dispersions				Vesicles		
R_t	30	15	5	2	∞	15 [a]	15
$V_{calculated}$	11	12 2	19 8	17 3	10 1	12 2	12 2
$V_{experimental}$	(8 3)	17 8 [b]	17 9	2 1	7 7 [c]	28 17 [c]	14 2 [b]

[a] Without incubation at $T > T_m$

[b] Values reduced by about 50% are found for the discoidal symmetry

[c] Values corrected for the existence of an internal water volume

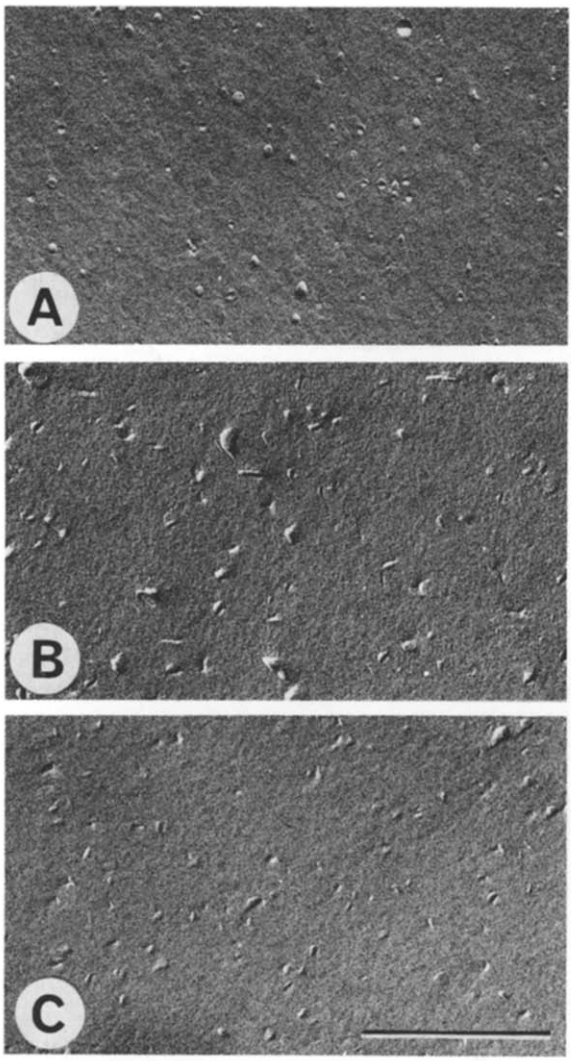

Fig 7 Freeze-fracture electron micrographs of DPPC sonicated vesicles with and without added melittin, freeze-fractured from 20°C (A) Pure DPPC vesicles (B) $R_t = 15$ without incubation (C) $R_t = 15$ after incubation of the mixture at 50°C Magnification 50000×

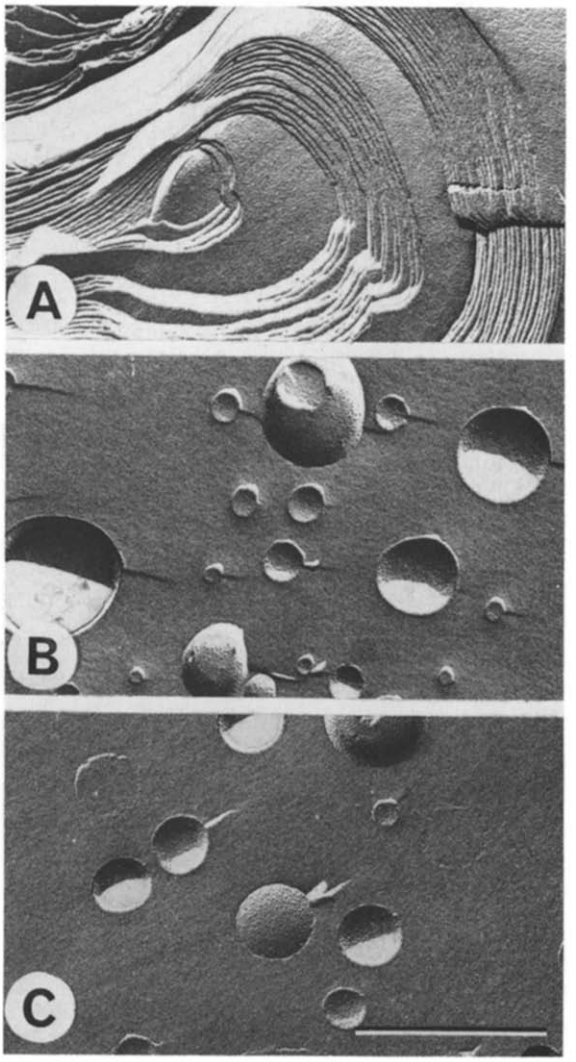

Fig 8 Freeze-fracture electron micrographs of egg PC dispersions in the presence and absence of melittin $T = 20$°C (A) Pure lipid dispersions, (B) $R_t = 30$, (C) $R_t = 15$ Magnification 50000×

tween melittin and vesicular DPPC, in contrast to the absence of any visible interaction with large multilamellar DPPC liposomes (Fig 6A) When the same sample is incubated at 50°C and frozen from 20°C, the small flat objects are formed (Figs 7C, 10a), very similar to those observed previously with the equally treated DPPC dispersions (Fig 6C)

When mellitin is added to egg PC dispersions, the initial large multilamellar liposomes (Fig 8A) are broken into large, heterogeneous in size, mostly unilamellar vesicles (Fig 8B) The heterogeneity of the samples decreases with the increased amount of melittin added, at $R_t = 15$ for example, the mean diameter of vesicles is 1730 ± 300 Å (Figs 8C and 10b) Contrary to the smooth appearance of pure PC dispersions (Fig 8A) and unilamellar

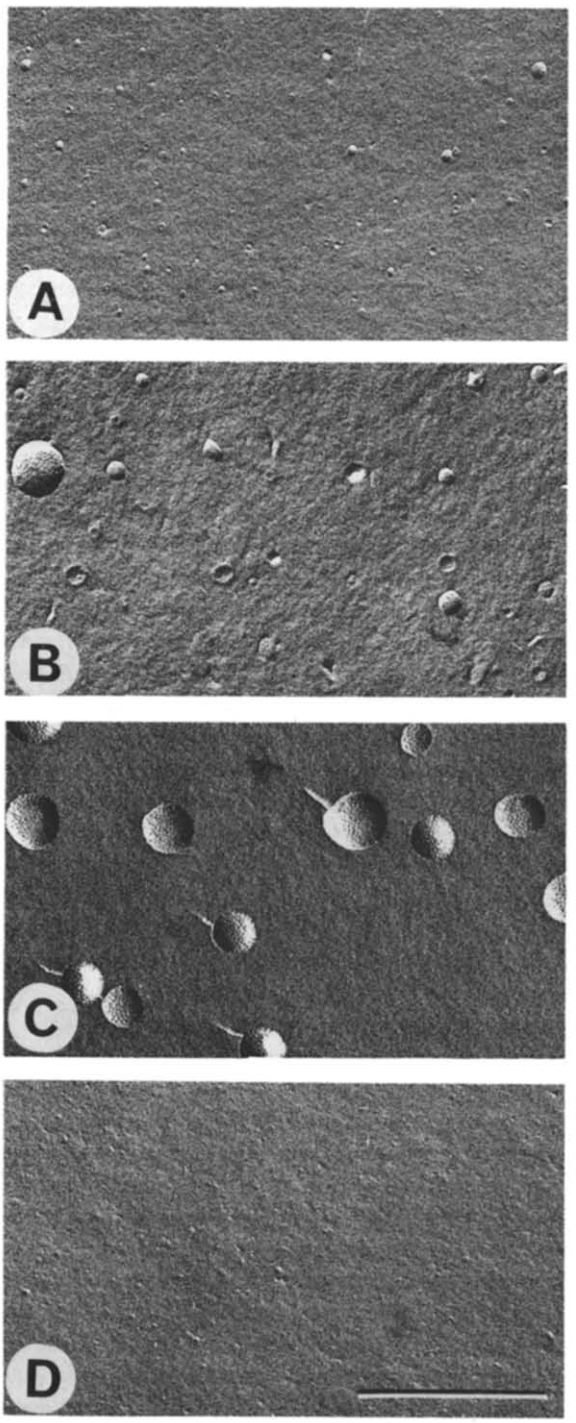

Fig 9 Freeze-fracture electron micrographs of egg PC vesicles in the presence of increasing amounts of melittin $T = 20\,°C$ From top to bottom (A) pure EPC vesicles, (B) $R_t \simeq 200$, (C) $R_t = 30$ (D) $R_t = 5$ Magnification 50000×

vesicles (Fig 9A), the melittin-lipid vesicles always display rough fracture surfaces (Figs 8B, 8C and 9C)

When melittin is added to small, sonicated egg PC vesicles (Fig 9A), complex behaviour is observed The small amounts of melittin induce a fusion of the egg PC vesicles into larger ones, leading to heterogeneous population of vesicles (Figs 9B and 10b) This heterogeneity is minimal for $R_t \cong 30$, where vesicles of $\phi = 1300 \pm 300$ Å are observed (Fig 9C and the histogram in Fig 10b) When more melittin is added, the vesicles are transformed into small flat objects (Fig 9D)

Discussion

The most general result of this study is that melittin exhibits strong interactions with lipids and is able to change the structure of lipid bilayers displaying liquid-like, α, conformation of their hydrocarbon chains In contrast, melittin lack appreciable interaction for the same lipids displaying rigid, β or β', conformation of their hydrocarbon chains, with the very interesting exception of sonicated small vesicles of DPPC

The structure of the new supramolecular melittin-phospholipid compexes depends on (i) the lipid-to-protein molar ratio, R_t, or, more exactly, the real lipid-to-peptide molar ratio (R_c) within the complex, (ii) whether the lipid chains are ordered or not

Comparison of the results obtained by different techniques

Light scattering, gel filtration and freeze-fracture electron microscopy reveal different but complementary aspects The relationship between the Stokes radii obtained by gel-filtration and the mean diameters measured by freeze-fracture electron microscopy has recently been established [24] As seen in Table III, qualitative agreement exists on the size of the melittin-lipid complexes formed However each technique has its own drawback Gel-filtration implies dilution and risk of dissociation of complexes onto the column, moreover, Sepharose 4B does not allow fractionation of large particles Freeze-fracture electron microscopy permits in principle, detection of all types of particle having a size larger than about 50 Å, this is

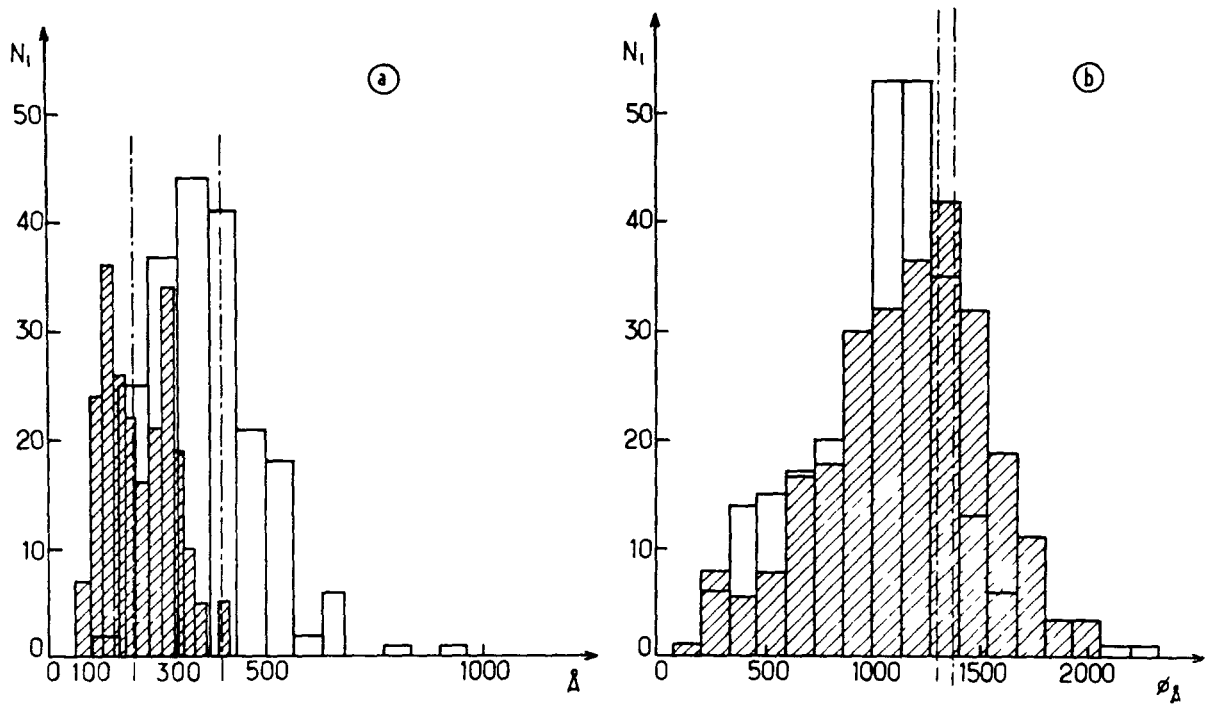

Fig 10 Histograms of size distribution of PC-melittin complexes measured from freeze-fracture electron micrographs (a) DPPC vesicles + Mel, $R_t = 15$, without (□) and with (▨) incubation at 50 °C (b) DPPC dispersions + Mel $R_t = 30$, at 50 °C (▨), egg PC vesicles + Mel, $R_t = 30$, at 20 °C (□) The vertical lines are the mean size in number for each distribution

illustrated in the case of well-defined particles as seen in Fig 10 It also clearly demonstrates that heterogeneous systems are formed at low melittin content Quasi-elastic light scattering, which is very sensitive to polydispersity, mainly detects the largest molecular weight particles, as already documented for pure lipid vesicles [22] Then, since for $R_t = 30$ the size of vesicles differ very significantly according to the technique used, more confidence was given to the mean value obtained by electron microscopy, $\phi \cong 1300 \pm 300$ Å for egg PC (Fig 10b) A small fraction of large vesicles,

TABLE III

HYDRODYNAMIC RADII, R_H (IN Å), OF PARTICLES IN SOLUTION AS MEASURED BY THE THREE TECHNIQUES LIGHT-SCATTERING (QELS), FREEZE-FRACTURE ELECTRON MICROSCOPY (EM) AND GEL-FILTRATION OF SEPHAROSE (GPC)

	DPPC-Mel					EPC-Mel					DMPC-Mel	DMPC-Apo A_{II}		DMPC-Glucagon
R_t	3	5	15	30	30 [b]	3	5	15	30	200	15 [c]	d	e	f
QELS	65	75	110	140	2000 [a]	41	60	1400 [a]	1000	650		65	55	
EM	60	90	96	94	690		41	1040 [a]	650 640 [a]	275		105	78	107
GPC		66	70 [a]	79			37	51 [a]	44		69			

[a] Value obtained when lipid was initially in MLV
[b] Experiment done at 50 °C
[c] Experiment done at 10 °C
The data for Apo A_{II} at 20 °C (d) and 30 °C (e) are from Massey et al [33,34], those for glucagon (f) from Jones et al [35]

such as those occurring on the edge of the distribution, in Fig 10b, will be sufficient to dominate the scattered intensity and significantly mask the dominant number of smaller vesicles A similar problem occurs for DPPC vesicles at $R_i = 30$ in the fluid phase On the other hand all techniques agree (Table III), due to lesser polydispersity at higher amounts of melittin, when small particles are formed

Morphological changes induced by melittin on lipid bilayers

When the hydrocarbon chains of the lipids are in the fluid, α, conformation, the interaction between melittin and dispersions or sonicated lipid vesicles leads to identical final lipid-melittin complexes When the hydrocarbon chains are ordered, only sonicated vesicles show morphological changes However, after incubation at $T > T_m$, new structures are then observed even below T_m, regardless of the initial state of the lipids (SUV or MLV)

On varying the amount of melittin added to lipid bilayers different processes occur At high R_i values, i e , low melittin content, heterogeneous systems are always observed, with the coexistence of unperturbed lipids and new lipid-peptide structures (cf Figs 6B, C and 9B) When melittin is added to lipids in their fluid state, and $12 < R_i < 50$, the complexes are single unilamellar vesicles of about 1300 ± 300 Å diameter (Table III) For lipids in the gel phase, at $R_i < 50$, very different structures are formed, since particles with R_H varying from 95 to 60 Å are observed (Table III) Similarly, for egg PC at $R_i < 12$, small species are observed with R_H values ranging from 95 to 40 Å Freeze-fracture indicates that the DPPC-melittin complexes resemble flat discoidal particles at $R_i = 15-30$ and become more spherical upon decreasing R_i

The composition of such discs remains roughly constant in the limit of experimental error at $R_c = 20 \pm 5$, when R_i varies from 15 to 5 (Table I) At variance, egg PC-melittin complexes have an R_c varying along the elution profile, which could reflect more labile structures dissociating onto the column The approximate size of the discoidal particles can be determined from the electron micrographs (Fig 10a) Their thickness is best estimated on the objects fractured perpendicularly to the plane of the discs and shadowed at highest angles The comparison of such measurements with those obtained with cross-fractured liposomes indicates that the discs are approximately one bilayer thick The thickness of the hydrated bilayer of DPPC in the gel phase ($e \cong 55$ Å) permits calculation of the diameter of the flat disc using equations already developed for PC/bile salt mixtures [25] For $R_i = 15$ at 20°C, using a mean value $R_H = 101$ Å (Table III), one obtains the disc diameter, $\phi \cong 235 \pm 23$ Å Finally, for high melittin amounts ($R_i < 5$), very small, almost spherical, complexes are always formed At $R_i = 3$, their radii are 60 Å for DPPC and 40 Å for egg PC (Table III) and one can propose that they correspond to mixed micelles The overall evolution of the morphology of lipids in the presence of increasing amounts of melittin can therefore be summarized as shown in Fig 11

Our data on changes in size and shape have to be compared to those of Prendergast et al [11] who observed disc-shaped particles at low melittin content ($40 < R_i < 160$) and large-sized ones at high melittin content ($R_i < 20$) The fact that we observed the opposite behaviour may be due to the possible contamination of melittin used by these authors by trace amounts of phospholipase

As evidenced in our study by freeze-fracture electron microscopy and light-scattering, fusion processes are clearly occurring upon addition of melittin to sonicated vesicles, since large unilamellar vesicles of several thousand ångstroms diameter are stabilized at high R_i values It implies that a significant percentage of SUV merge into a single new structure Such a melittin-induced fusion process has already been reported on SUV constituted by PC-cardiolipin mixtures and resulted in the formation of very large MLV, of several micrometers diameter [13] Our results also agree with the more documented study by Morgan et al [12], who showed that melittin even at $R_i \cong 200$ can induce the fusion of large unilamellar vesicles (LUV) by going through the transition temperature domain of DPPC

It has to be emphasized that, for lipids in the fluid state, the fusion process of SUV leads to the formation of large, mostly unilamellar vesicles, similar to those obtained by the melittin-induced

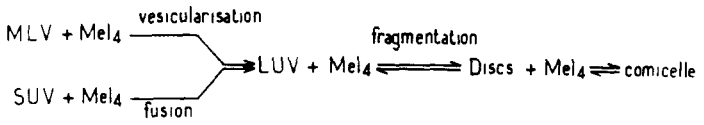

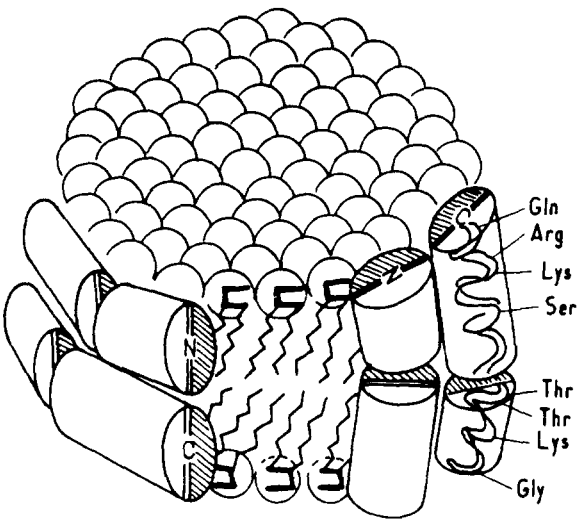

Fig 11 Summary of successive events in changing the morphology of lipid bilayers in the presence of increasing amounts of melittin, for $T > T_m$ LUV is used for large unilamellar vesicles Below, a drawing of the tentative models proposed for discoidal complexes formed by melittin with DPPC at $T < T_m$ Main features derived from disc models already proposed for lipoproteins [28,32], the principal characteristics of melittin derived from X-rays [38] have been maintained Hatched area of melittin corresponds to the hydrophobic face of the amphipathic helix

disruption of large multilamellar liposomes Therefore, it seems that such large vesicles represent a thermodynamically stable structure for fluid lipid-melittin complexes at high R_c values

Our data also compare well with previous results obtained with some other proteins [28–34] or peptides [35,36] having amphipathic helices and which were shown to induce breakdown of vesicles into discoidal particles of similar size (Table III) Staphylococcal δ-lysin, which has a structure and properties closely related to those of melittin [26], has recently been mentioned as inducing the formation of particles on the fracture plane of lipids and fragmentation into discoidal objects [27]

Structure of discoidal complexes

Segrest [28] first developed the so-called 'bicycle tyre model' to account for the structure of discoidal lipid-peptide complexes In such a model, lipids are organized as an area of bilayer limited at its periphery by a single belt of peptides parallel to the surface of the bilayer In order to be applied to melittin, one has to define the shape and size of the peptide From X-ray studies [2,37] one can assume that melittin is a rod of about $\phi_{mel} = 12 \pm 1$ Å diameter and a length, L_{mel}, of 35 ± 5 Å In the gel state, lipid molecules packed in a bilayer occupy an area of $S_{PL} = 50$ Å^2 With these hypothesis and a diameter of the discs $\phi = 235 \pm 23$ Å, for $R_t = 15$ at 20°C, one can calculate the number of lipid molecules within one disc to be about $N_{PC} \cong 1400 \pm 300$ The number of peptides needed to generate a belt of amphipathic helices with their axis parallel to the plane of the bilayer is $N_p = 20 \pm 5$ This corresponds to a ratio, $R_c = N_{PL}/N_P \cong 70 \pm 30$, that is significantly higher than the experimental value, $R_c \cong 20 \pm 5$, found by gel-filtration In order to account for our experimental results with such a tyre model, one can add a second belt of melittin molecules (as shown in Fig 11), which leads to $N_p = 40 \pm 10$ and to $R_c \cong 35 \pm 15$ This value is still higher than the experimental one

On the other hand, the melittin rod can be positioned differently A better packing of α-helix rods is offered when the melittin is perpendicular to the bilayer plane, as shown in Fig 11 With such a model, as already proposed for apolipoprotein by Tall et al [32], and using the same data as above, one obtains $N_P = 61$ and $R_c = 25 \pm 7$ This

value agrees well with the observed one

The first possibility, with melittin forming a 'double tyre' parallel to the lipid bilayer (Fig 11) looks, in fact, very similar to that speculated by Terwilliger et al [38], and could correspond to the layers of melittin dimers that have been described by X-rays in the crystal of pure melittin The second possibility, with melittin perpendicular to the bilayer, would agree with the conclusions of Vogel et al [8] Due to uncertainty in the size melittin bound and in the values of R_c and the disc diameter, one cannot definitively discriminate between the two models, which are perhaps only extreme cases of the real situation However, the model with perpendicular, or tilted, melittin, which can account for lower R_c values, fits better the experimental data

It has to be emphasized that light-scattering and freeze-fracture data indicate a continuous decrease of R_H versus R_1 The disc diameter goes from 140 Å at $R_1 = 30$ to 75 Å for $R_1 = 5$ Such large and progressive changes imply that more melittin becomes bound and R_c decreases, it results that melittin rod has to accommodate such a progressive decrease in the belt diameter The perpendicular model allows easily such an evolution

Flat objects have also been detected when melittin interacts with DPPC vesicles in the gel phase without incubation at 50°C In that case the diameter observed $\phi \cong 356$ Å at $R_1 = 15$ (Fig 8b) is nearly twice as highly as the one observed after incubation above T_m, as discussed above This is probably due to the fact that no redistribution of the lipids can occur in the gel phase, contrary to what happens on going through T_m Due to uncertainties concerning the value of this diameter, but mainly in the thickness of the flat objects, it is rather difficult to conclude whether such objects are flat discs with a single bilayer or flattened vesicles The first hypothesis supposes a total opening of the initial SUV and implies again that the rims are coated by melittin, in the second hypothesis the flattening will be due to insertion of melittin, which locally severely decreases the curvature radius, and then acts as a wedge, a mode of action of melittin first proposed by Dawson et al [39] Such a structure has already been proposed for ApoCIII-PL systems [28]

Reinterpretation of the lipid perturbations in the light of morphological changes

Using the above conclusions, one can also discuss the perturbations of the thermotropic behaviour of lipids induced by melittin [4–6, 40] It has been shown [5] that increasing amounts of melittin induce a progressive broadening of the lipid phase transition and a 10°C downwards shift of its temperature Due to the very similar conditions in which these effects occur compared to the presence of discs, one can propose that such effects on the lipid thermotropism can be interpreted as reflecting changes (i) in the amount of the different phases which coexist for $R_1 > 15$, as shown by freeze-fracture data (Fig 6B), (ii) in the size of discoidal particles, for $R_1 < 15$, which could result in a lower cooperativity of the transition The disappearance of any transition at $R_1 \cong 2$ [43] can also be related to the decrease in size of the objects, which are then probably too small to accommodate lipids in a bilayer structure

Implications of the morphological changes on the mechanism of membrane lysis induced by melittin

When summarizing the observed effects, as shown in Fig 11, the redistribution of lipids and peptide into new structures in model systems illustrates many events analogous to those involved in biological membrane functions That is fusion processes, which are constructive events, but also it seems that melittin is an especially suitable peptide for fragmentation of membranes, which could occur in two steps vesicularization, and formation of discoidal small particles

Such conclusions may be of some interest for understanding the melittin-induced membrane lysis When dispersions are fragmented into vesicles, it implies that the lipids have been taken off the 'mother' membrane by melittin, in agreement with conclusions of Sessa et al [9] There could result 'holes' that are large enough to account not only for changes in ionic permeabilities but also for leakage of larger molecules such as proteins and nucleic acids At low melittin content and for lipids in their fluid phase, such transient holes can rapidly be annealed by lateral diffusion This could correspond to the early, sudden increase in ionic or small solute permeability At higher melittin contents, and/or with less mobile lipids, statisti-

cally larger holes could have a longer lifetime, so that large species would leave the cell Such a sequence of events agrees with that already observed on model membrane [9,40] and proposed for the release of cell components [42,44] The formation of discs or co-micelles, which indicates a major detergent effect on the membranes, would probably be the last step of cell lysis

Consequences of the morphological changes on the synergism between melittin and phospholipases

Melittin is well known to increase the activity of phospholipases In the case of egg PC SUV and *Escherichia Coli* cell membranes, this increase, up to 6-fold, depends on the melittin-to-lipid ratio [45] In the case of egg PC dispersions, the rate of enzymatic reaction increases proportionally to the amount of added melittin up to a 300-fold factor for $R_i = 16$ [46] Since in the same R_i range we demonstrate that melittin changes egg PC dispersions into single unilamellar vesicles of large diameter, we suggest that this drastic increase in phospholipase activity is simply related to the total exposure of the lipid molecules to the enzyme It has to be emphasized that there remains to be explained a 2- to 6-fold increase in phospholipase A_2 activity on SUV and natural membranes, which is probably due to a more subtle change in the lipid structure in the presence of melittin

Our observation of the rough fracture surfaces appearing on the melittin-PC vesicles may well reflect such a perturbation of the local lipid structure Such rough surfaces have been found mainly for transmembrane proteins or hydrophobic peptides which can span the lipid bilayer [23] Even if they have also been observed for lipid mixtures when different phases coexist [47], the occurrence of such defects both on DPPC and egg PC vesicles has never been observed Then it could be concluded that melittin really interacts deeply with the lipids, and such a conclusion agrees with the recent finding that it can perturb the structure of methylene groups in the core of the bilayer, as detected by deuterium NMR [48]

Acknowledgements

We would like to thank J C Dedieu, C G M, Gif sur Yvette, for his excellent technical assistance throughout this investigation

References

1 Habermann, E, (1980) in Natural Toxins (Eaker, D and Wadstrom, T eds) pp 173–181, Pergamon Press New York
2 Terwilliger, T C and Eisenberg, D E (1982) J Biol Chem 257, 6016–6022
3 Brown, L R, Braun, W, Kumar, A and Wuthrich, K (1982) Biophys J 37, 319–328
4 Bernard, E, Faucon, J F and Dufourcq, J (1982) Biochim Biophys Acta 688, 152–162
5 Dasseux, J L, Faucon, J F, Lafleur, M, Pézolet, M and Dufourcq, J (1984) Biochim Biophys Acta 775, 37–50
6 Jahnig, F, Vogel, H and Best, L (1982) Biochemistry 21, 6790–6798
7 Talbot, J C, Lalanne, J, Faucon, J F and Dufourcq, J (1982) Biochim Biophys Acta 689, 106–112
8 Vogel, H, Jahnig F, Hoffmann, V and Stumpel, J (1983) Biochim Biophys Acta 733, 201–209
9 Sessa, G, Freer, J H, Colacicco, G and Weissmann, G (1969) J Biol Chem 244, 3575–3582
10 Lavialle F Levin, I and Mollay, C (1980) Biochim Biophys Acta 600, 62–71
11 Prendergast, F G Lu J, Wei, G J and Bloomfield V A (1982) Biochemistry 21, 6963–6971
12 Morgan C G Williamson, H, Fuller, S and Hudson, B (1983) Biochim Biophys Acta 732, 668–674
13 Eytan, G D and Almary, T (1983) FEBS Lett 156, 29–32
14 Weibel, E R and Bolender, R P (1973) in Principles and Techniques of Electron Microscopy, Vol 3 (Hayat, M A, ed), Ch 6, Van Nostrand Reinhold New York
15 Le Maire, M, Rivas E and Moller, J V (1980) Anal Biochem 106, 12–21
16 Dasseux, J L (1983) These de 3ème cycle, Université de Bordeaux I
17 Koppel, D E (1972) J Chem Phys 57, 4814–4820
18 Podo, F, Strom, R, Crifo, C and Zulauf, M (1982) Int J Pept Res 19, 514–527
19 Faucon, J F, Dufourcq, J and Lussan, C (1979) FEBS Lett 102, 187–190
20 Gulik-Krzywicki, T, Aggerbeck, L P and Larsson K (1984) in Surfactants in Solution (Mittal, K L and Lindman, B, eds), pp 237–257, Plenum Press, New York
21 Gulik-Krzywicki, T and Costello, J (1978) J Microsc 112 103–113
22 Wong, M and Thompson, T E (1982) Biochemistry 21, 4133–4139
23 Gulik-Krzywicki T (1975) Biochim Biophys Acta 415, 1–28
24 Le Maire M, Moller, J V and Gulik-Krzywicki, T (1981), Biochim Biophys Acta 643 115–125
25 Mazer, N A Benedek, G B and Carey, M C (1980) Biochemistry 19, 601–615
26 Bhakoo, M, Birkbeck, T H and Freer, J H (1985) Canad J Biochem 63, 1–6
27 Freer, J H, Birkbeck, T H and Bhakoo, M (1984) in Bacterial Protein Toxins, (Alouf, J E, Fehrenbach F J, Freer J H and Jeljaszewicz, J eds), pp 181–189, Academic Press, New York

28 Segrest J P (1977) Chem Phys Lipids 18, 7–22
29 Atkinson D Smith, H M Dickson, J and Austin J P (1976) Eur J Biochem 64, 541–547
30 Middelhoff, G , Rosseneu, M , Peeters, H and Brown W V (1976), Biochim Biophys Acta 441, 57–67
31 Aune K C , Gallagher, J G , Gotto, A M and Morrisett J D (1977) Biochemistry 16, 2151–2156
32 Tall, A R Small, D M Deckelbaum, R J and Shipley G G (1977) J Biol Chem 252, 4701–4711
33 Massey, J B , Gotto, A M and Pownall H J (1981) Biochemistry 20, 1575–1584
34 Massey, J B Rohde M F Van Winkle, W B Gotto, A M and Pownall H J (1981) Biochemistry 20, 1569–1574
35 Jones A J S , Epand R M , Lin, K F , Walton, D and Vail W J (1978) Biochemistry 2301–2307
36 Epand R M Epand R F , Orlowski, R C , Schlueter R J Boni L T and Hui S W (1983) Biochemistry 22, 5074–5084
37 Gevod V S and Birdi, K S (1984) Biophys J 45, 1079–1083
38 Terwilliger, T C Weissman, L and Eisenberg, D (1982) Biophys J 37 353–361
39 Dawson, C R , Drake, A F , Helliwell J and Hider, R C (1978) Biochim Biophys Acta 510 75–86
40 Dufourcq, J , Dasseux, J L and Faucon J F (1984) in Bacterial Protein Toxins, (Alouf, J , Fehrenbach, F J , Freer, J H and Jelaszewicz, J , eds), p 127–138, Academic Press, New York
41 Epand, R M and Sturtevant, J M (1981) Biochemistry 20, 4603–4606
42 De Grado W F , Musso, G F Lieber, M , Kaiser, E T and Kezdy F J (1982) Biophys J 37 329–338
43 Faucon, J F , Dasseux J L , Dufourcq, J Lafleur M , Pezolet, M , Le Maire, M and Gulik-Krzywicki, T (1986) in Surfactants in Solution, (Mittal, K L and Bothorel P eds), Plenum Press New York, in the press
44 Thelestam, M and Mollby R (1979) Biochim Biophys Acta 557 156–169
45 Mollay, C and Kreil, G (1974) FEBS Lett 46, 141–144
46 Yunes, R , Goldhammer, A R , Garner, W K and Cordes E H (1977) Arch Biochem Biophys 183, 105–112
47 Verkleij A J Mombers, C Leunissen-Bijvelt, L and Ververgaert, P J J (1979) Nature 279 162–163
48 Dufourc, E J Smith I C P and Dufourcq J (1986) in Surfactants in Solution, (Mittal K L and Bothorel, P eds), Plenum Press, New York in the press